STUDY OF AASHO LOADINGS ON A CONCRETE BOX GIRDER BRIDGE MODEL

A. C. Scordelis and J. G. Bouwkamp, University of California, Berkeley; and S. T. Wasti, Middle East Technical University, Ankara, Turkey

A brief description of the instrumentation, construction, and testing of a large-scale, two-span, four-cell, reinforced concrete box girder bridge model is presented. Tested in the laboratory, the model was a 1:2.82 scale of a typical prototype bridge found in the California highway system. The overall plan dimensions of the model and the prototype were 12 by 72 ft and 34 by 203 ft respectively. The research program included a study of the theoretical and experimental response of the bridge to dead load, live loads at working stress and overstress levels, and ultimate loading to failure. However, this paper presents only the results of the investigation dealing with an evaluation of present AASHO loadings on bridges of this type and the response of the bridge to actual scaled loads of AASHO HS20-44 trucks placed in two or three lanes and of a proposed class I overload construction vehicle placed in one lane only. Results indicate that concrete box girder bridges have excellent load distribution properties; however, the present AASHO empirical formula, which ignores the number of lanes on the bridge, underestimates the true value for three lanes of trucks. Total stresses in the steel and concrete under three lanes of AASHO trucks or one lane of the overload vehicle exceed allowable values, but no distress in the bridge was observed. /AUTHOR/

•IN 1971, approximately 80 percent of the concrete bridges (computed on the basis of deck area) in California were multicell concrete box girder bridges. These cast-in-place structures are usually constructed as reinforced concrete bridges with spans ranging between 60 and 100 ft and as post-tensioned prestressed bridges for longer span lengths.

Because of their large use in California, a continuing program of research on box girder bridges, directed toward improved design methods, has been conducted at the University of California, Berkeley, since 1965. Simple and continuous straight bridges, skew bridges, and curved bridges are successively being studied through use of analytical and experimental methods.

As part of this research program, an extensive investigation was carried out on the structural behavior of the large-scale, two-span, reinforced concrete box girder model shown in Figures 1 and 2. The model, having overall plan dimensions of 12 by 72 ft, was a 1:2.82 scale replica of a typical prototype bridge, 34 by 203 ft, found in today's California highway system. It had four cells: a center bent with a single column support, two end diaphragms, and, for purposes of comparison, a midspan diaphragm at section X but not at section Y. The large scale of the model enabled the use of standard high-strength (60-ksi yield) deformed steel bars as reinforcement and concrete with $\frac{3}{8}$-in. aggregate rather than a mortar mix for the model material. The model was tested in the Structures Laboratory at the University of California.

Three research reports (1, 2, 3) describe in detail the model dimensions and reinforcement, method of construction, instrumentation, automatic data recording and

Sponsored by Committee on Concrete Superstructures.

Figure 1. Dimensions of box girder bridge model with transverse locations.

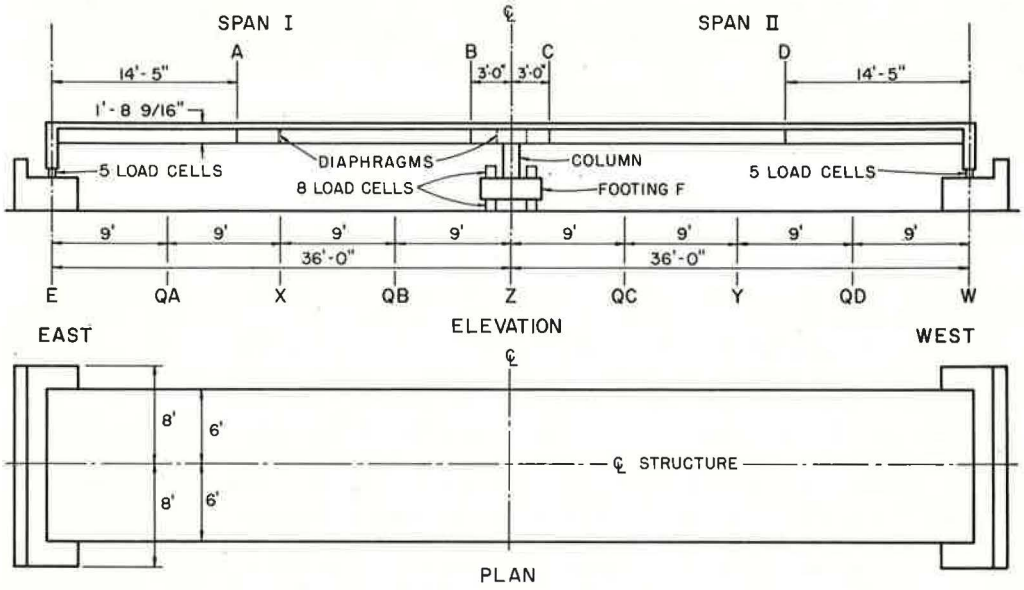

Figure 2. Cross section of box girder bridge model.

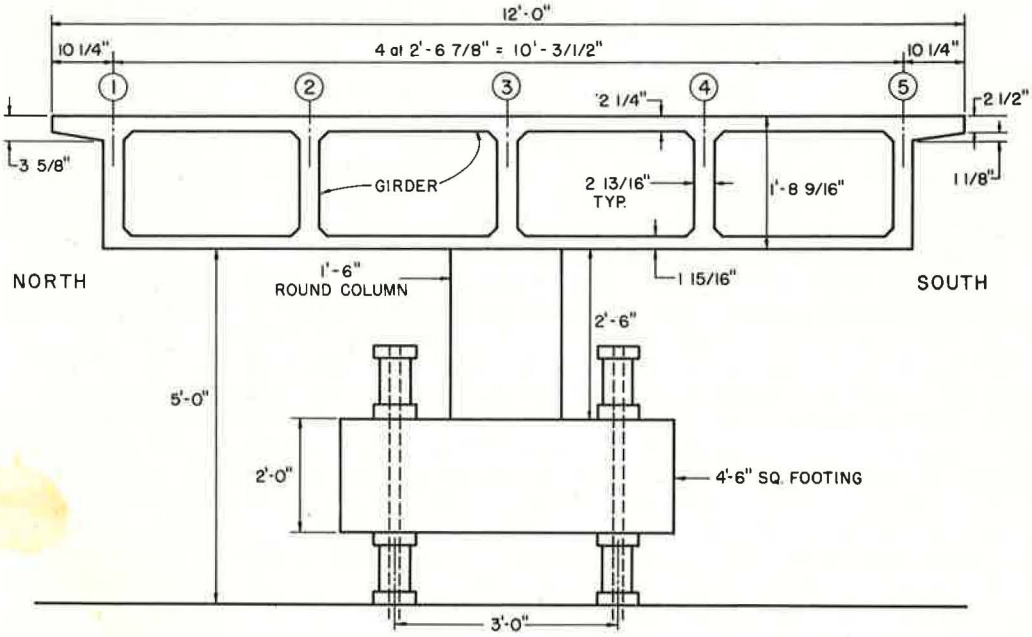

reduction system, and test program. Also presented are theoretical and experimental results for the response of the bridge to dead load, live loads at working stress and overstress levels, and ultimate loading to failure. Theoretical results for working stress loads were based on a finite element analysis assuming the structure to be an uncracked, homogeneous, elastic structure.

The purpose of this paper is to present only the results of the investigation dealing with an evaluation of the present AASHO loadings on bridges of this type.

EXPERIMENTAL PROGRAM

The same procedure used in the field on prototype structures was used to construct the model. The two end abutments and the center column and footing were cast first. Subsequently, the bottom slab, girder webs, and diaphragms at section X and at the center bent Z were formed, reinforced, and cast. At this stage, to satisfy similitude for dead load, we placed extra dead weight in the form of steel billets in the cells. The billets plus the dead load of the model resulted in the required model-prototype weight ratio of 1:2.82. The top slab was then formed, reinforced, and cast.

Instrumentation was designed to measure reactions, deflections, and strains in the concrete and the steel reinforcement. Reactions were measured by load cells at each of the five girders, numbered 1 to 5 (Fig. 2) at the two end abutments and at four locations under the central footing. Vertical deflections were measured by potentiometers at each girder web at transverse sections X, QB, Z, QC, and Y (Fig. 1). Longitudinal strain was measured with strain meters in the concrete and with weldable waterproof gauges on the steel reinforcement at sections A and D in the maximum positive moment region and at sections B and C near the center support in the negative moment region. All data recording and reduction were automated as much as possible using available computer systems.

The main objective of the test program was to obtain information on load distribution in reinforced concrete box girder bridges under conditions of working loads. Working loads would result in total design stresses of 24 ksi in the tensile steel at the sections of loading. Bearing in mind, however, that the tensile stresses in the tensile reinforcement at these sections due to their own weight and extra dead load of the bridge model alone were about 12 ksi, we decided to consider two levels of working loads: those producing total stresses in the steel of 24 ksi and those resulting in total tensile steel stresses of 30 ksi at the sections of loading. The advantage of the latter stress level was that 50 percent higher live load stress and strain values could be registered for a total increase in the bridge model stresses of only 6 ksi.

In terms of actual experimental data, it was convenient to divide the experimental program into seven phases, from the dead load condition (phase 0) through the 24, 30, 40, 50, and 60 ksi stress levels (phases 1 to 5) to the failure condition (phase 6).

The box girder bridge model had a loading frame at midspan sections X and Y enabling live loads to be applied at each of the girders 1 to 5 by means of jacks singly and in various combinations (Fig. 3). Each phase of the experimental program for live loads comprised first the application of equal loads on each girder at both midspans to produce the same order of nominal steel stress at sections of maximum positive and negative moment. These loads were termed "conditioning loads." Subsequently, after the removal of the conditioning loads, point loads were applied in several combinations. The conditioning loads were chosen to produce nominal total tensile steel stresses of 24, 30, 40, 50, and 60 ksi at the sections of loading and to represent the successive deterioration of the box girder bridge model due to the effects of overload. The point loads, however, were chosen in all cases to produce stresses where applied on the order of the working stresses, i.e., 24- and 30-ksi total tensile stress in the reinforcement.

The working load phase, which involved the application of the conditioning loads to produce the 30-ksi tensile steel stress, was chosen as the most representative from the point of view of assessing actual box girder bridge behavior for design purposes. Following the conditioning loads, 19 separate single or combined point load combinations were applied to the bridge model at midspan sections X and Y. Results from these point loads could then be used to develop influence tables for reactions, deflections,

strains, stresses, and moments. In addition, during this working load phase, the model was subjected to scaled-down versions of the wheel loads from standard AASHO HS20-44 trucks and a proposed class I overload construction vehicle. Dimensions and wheel loads of prototype and model vehicles are shown in Figures 4 and 5. Six AASHO trucks and two construction vehicles were fabricated using a system of statically determined beams. Figure 6 shows a three-lane AASHO truck loading on the bridge model and indicates how the resultant of each truck's wheel loads was applied through a single jack. A variety of vehicle loading patterns was used and will be described in detail later.

MAXIMUM NUMBER OF WHEEL LOADS CARRIED BY A GIRDER

Present AASHO specifications prescribe a design method wherein a box girder bridge is considered to be made up of a number of identical I-shaped interior girders plus two exterior girders. According to these specifications, each girder is designed as a separate member by applying to it a certain fraction of a single longitudinal line of wheels from the standard truck. This fraction, known as the number of wheel loads N_{WL}, is given for interior girders as

$$N_{WL} = S/7$$

and for exterior girders as

$$N_{WL} = S_1/7$$

where S is the flange width in feet of the interior girder, which is equal to the average width of the cell, and S_1 is the top flange width in feet of the exterior girder, which is equal to half the cell width plus the cantilever overhang. In December 1967 the state of California put forward a design specification in which the distinction between S_1 and S was abolished and the total value of the distribution factor N_{WL} for the "whole-width unit" was given by

$$N_{WL}(\text{total}) = \frac{\text{deck width in feet}}{7}$$

It has been pointed out (2) that the most important variable not taken into account by the AASHO specifications is the number of traffic lanes on the bridge. Other factors such as span, total width, number of cells, and continuity or fixity at the supports also influence the load distribution.

The prototype bridge represented by the model could be either two- or three-lane depending on the choice of barrier curb and railing used. Theoretical and experimental load distributions were determined as described below.

The actual box girder cross section was first divided into three interior girders (2, 3, and 4) and two exterior girders (1 and 5). The girder moment at any section taken by an individual girder was found by integrating the longitudinal stresses over the proper slab, web, or reinforcement areas to obtain forces and then by multiplying these forces by their respective lever arms to the neutral axis of the gross uncracked section. The girder moments, at a particular section, were summed to determine the total moment on an entire cross section. Each girder moment was then divided by the total moment at a section to determine the percentage distribution to each girder.

Theoretical and experimental percentages of the total moments at sections A, D, B, and C carried by each girder were computed for all 19 point load combinations applied at midspan sections X and Y. These gave essentially influence tables, which at a glance enabled determination of the load-distributing properties of the bridge. For an optimum load distribution, a uniform stress would exist across the entire section, and the percentage distributions to girders 1 to 5 would be 16.5, 22.4, 22.4, 22.4, and 16.5 percent respectively. These values are directly proportional to the gross moments of inertia of the interior and exterior girders.

To determine the maximum number of wheel loads carried by an interior or exterior girder at sections A, B, C, and D shown in Figure 1, we used the influence tables. Each

Figure 3. Loading frames with jacks in position.

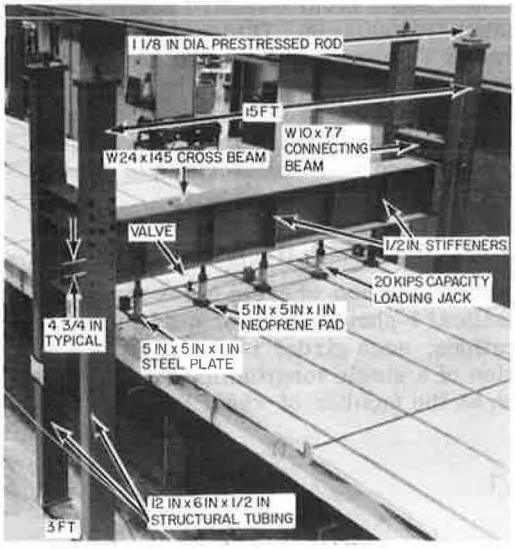

Figure 4. Wheel loads and dimensions of prototype and model AASHO HS20-44 truck.

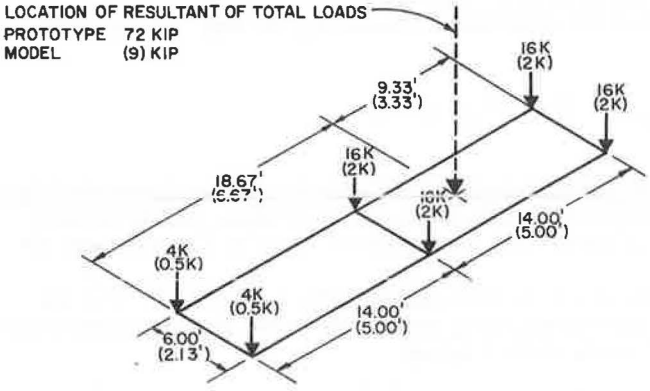

Figure 5. Wheel loads and dimensions of prototype and model overload construction vehicle.

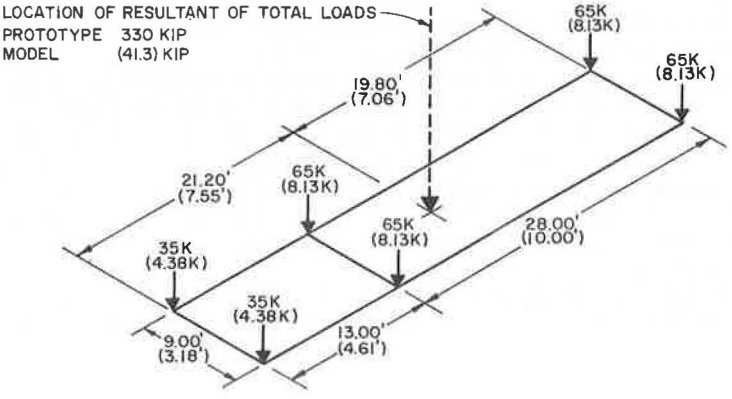

prototype AASHO truck was assumed to occupy a 10-ft traffic lane and have wheels spaced transversely at 6 ft. For simplicity, only a single transverse series of wheels at midspan sections X and Y were considered. For maximum positive moments at sections A and D only one span was loaded, whereas for maximum negative moments at sections B and C both spans were loaded.

Table 1 gives a summary of the results for the maximum number of wheel loads to be carried by interior or exterior girders at sections A, B, C, and D. Line 1 gives values computed from the AASHO formulas. The remaining lines give values for two lanes of trucks (total of four wheel lines on bridge) and for three lanes of trucks (total of six wheel lines on bridge). The uniform stress values (lines 2 and 5) are obtained by multiplying the total number of wheel lines on the bridge by 22.4 and 16.5 percent for the interior and exterior girders respectively. Theoretical values (lines 3 and 6) and experimental values (lines 4 and 7) are found by using influence ordinates as described above. Finally lines 8, 9, and 10 are given because AASHO specifies a 10 percent reduction for three lanes of loading. It is important to note that, in using the S/7 AASHO empirical formula, no reduction should be made for more than two lanes of loading because this is assumed to have been included already in the development of the formula.

A study of Table 1 reveals several interesting facts for the bridge under consideration:

1. The AASHO formulas are conservative for two-lane truck loading but unconservative for three-lane truck loading. The latter is especially true for interior girders, even with the 10 percent reduction, where AASHO underestimates the load by about 18 to 23 percent.
2. When theoretical and experimental values are compared, experimental values are 1 to 5 percent higher for interior girders at sections A, C, and D and 10 percent higher at section B. For exterior girders, differences of 2 to 3 percent exist at sections B and C and 5 to 14 percent at sections A and D.
3. When both theoretical and experimental values are compared with optimum uniform stress values, the former are generally only 2 to 8 percent higher than the latter, with three-lane truck loading being the closest. This emphasizes the excellent load-distributing properties of concrete box girder bridges.

AASHO TRUCK AND CONSTRUCTION VEHICLE LOADS

As described earlier, the model was loaded by scaled-down versions of the standard AASHO HS20-44 truck (total load = 72 kip) as shown in Figure 4 and a proposed class I overload construction vehicle (total load = 330 kip) as shown in Figure 5. All linear dimensions were reduced by the scale factor 1:2.82. Similitude required that the loads be reduced by a factor of 1:8 to produce the same stresses in the model as in the prototype. Thus, for the model the total load for each truck was 9.0 kip and for each construction vehicle was 41.3 kip. With these loads, a study could be made of the bridge response due to actual design truck live loads placed at various positions on the bridge.

Figure 7 shows the various positions and directions of the truck and construction vehicle loads on the bridge. A total of 11 combinations of two-lane truck loadings, three combinations of three-lane truck loadings, and seven combinations of construction vehicle loading were used. For the AASHO truck loadings it was assumed that one, two, three, four, or six trucks could occupy any of the positions shown in Figure 7. However, it was assumed that no more than one overload construction vehicle could be in each span at any one time because this would be a controlled loading. Reactions, girder moments, deflections, strains, and stresses were determined experimentally for all load combinations and theoretically for selected cases through use of a finite element analysis.

Reactions

Excellent static checks were obtained, with the ratios of the sum of the reactions to the sum of applied loads varying from 0.97 to 1.01 for all cases. The agreement between theoretical and experimental total reactions at the east, center, and west supports was very close (Table 2) for several typical cases of AASHO truck loadings.

Figure 6. Three-lane truck loading on bridge deck model.

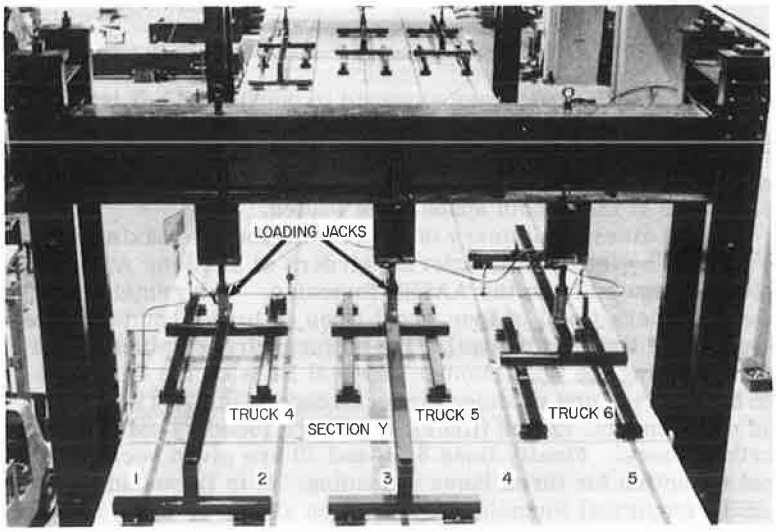

Table 1. Maximum number of wheel loads for interior and exterior girders.

Girder	Line	Load Case	Section A	B	C	D
Interior	1	AASHO specifications	1.04	1.04	1.04	1.04
	2	Two-lane (uniform stress)	0.90	0.90	0.90	0.90
	3	Two-lane (theoretical)	0.96	0.95	0.99	0.99
	4	Two-lane (experimental)	0.98	1.06	1.00	1.04
	5	Three-lane (uniform stress)	1.34	1.34	1.34	1.34
	6	Three-lane (theoretical)	1.37	1.38	1.40	1.39
	7	Three-lane (experimental)	1.42	1.54	1.45	1.47
	8	0.90 x three-lane (uniform stress)	1.21	1.21	1.21	1.21
	9	0.90 x three-lane (theoretical)	1.23	1.24	1.26	1.25
	10	0.90 x three-lane (experimental)	1.27	1.39	1.31	1.32
Exterior	1	AASHO specifications	0.88	0.88	0.88	0.88
	2	Two-lane (uniform stress)	0.66	0.66	0.66	0.66
	3	Two-lane (theoretical)	0.67	0.67	0.71	0.71
	4	Two-lane (experimental)	0.73	0.65	0.70	0.61
	5	Three-lane (uniform stress)	0.99	0.99	0.99	0.99
	6	Three-lane (theoretical)	0.96	0.95	0.97	0.97
	7	Three-lane (experimental)	1.02	0.94	0.99	0.84
	8	0.90 x three-lane (uniform stress)	0.89	0.89	0.89	0.89
	9	0.90 x three-lane (theoretical)	0.86	0.86	0.87	0.87
	10	0.90 x three-lane (experimental)	0.92	0.84	0.89	0.76

Figure 7. Positions and directions of truck and construction vehicle loadings on bridge.

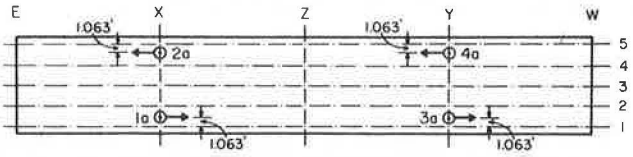

(a) TWO-LANE TRUCK LOADING (EACH TRUCK = 9.0 KIP NOMINAL)

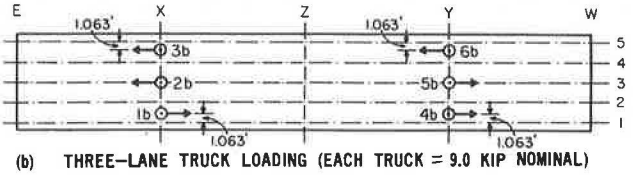

(b) THREE-LANE TRUCK LOADING (EACH TRUCK = 9.0 KIP NOMINAL)

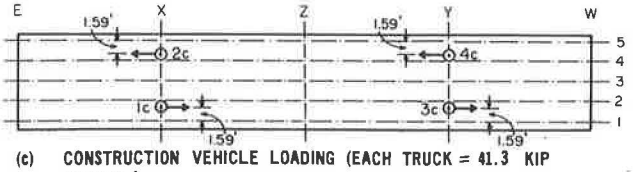

(c) CONSTRUCTION VEHICLE LOADING (EACH TRUCK = 41.3 KIP NOMINAL)

The good agreement indicates that the theory can also be used to accurately predict the total moment at any section of the bridge based on external reactions.

Girder Moments

Girder moments, total section moments, and percentage distributions to each girder were evaluated for the various vehicle load combinations using the procedure described earlier. Critical design vehicle positions for maximum experimental girder moments at each section are given in Table 3 together with the maximum moments in exterior and interior girders and their ratio. The following conclusions can be drawn:

1. As would be expected the maximum moments get progressively larger as one proceeds from two-lane truck to three-lane truck to construction vehicle loading because of the greater total load across the bridge width in each case.
2. When we consider positive moments at sections A and D, maximum moments are produced when only one span is loaded with as many vehicles as possible across the width of the bridge. Single vehicles in one span in an extreme eccentric position do not produce maximum effects.
3. When we consider negative moments at sections B and C, maximum moments are produced when both spans are loaded, again with as many vehicles as possible across the width of the bridge.
4. With the exception of two-lane AASHO loading for section D, where the exterior girder moment appears questionable, the ratios of maximum exterior to interior girder moments range from 0.61 to 0.76. For a uniform stress distribution across the bridge width this ratio would be 16.5/22.4 = 0.74.

Deflections

Experimental deflections are shown in Figure 8 for vehicle loadings that produce maximum values at diaphragmed section X and undiaphragmed section Y. For the two- and three-lane truck cases, the loading is relatively uniform across the width of the bridge (Fig. 7), which results in a uniform distribution of deflection also. For the construction vehicle, only one lane is loaded, which results in a larger deflection under girder 5. By comparing results at sections X and Y, these loadings also demonstrate the effect of the diaphragm.

It is of interest to compute the maximum deflection-span ratios for each of these design live loadings inasmuch as they would be the same in a full-scale prototype structure because of similitude. For the two-lane truck, three-lane truck, and construction vehicle loadings the maximum deflections are respectively 0.17, 0.25, and 0.51 in., which when divided by the span of 432 in. (36 ft) give deflection-span ratios of 1/2,600, 1/1,770, and 1/870, all of which are quite small.

A comparison of theoretical and experimental deflections, not shown, indicates that the theory predicts the general distribution of deflections quite well if the theoretical values based on an uncracked section are multiplied by a factor of about 1.5 to account for cracking at the working stress level.

Maximum Stresses

The maximum live load experimental stresses in the concrete and the steel reinforcement for all vehicle load positions considered are given in Table 4. These were obtained by searching all the measured strain values at each section under all vehicle load combinations studied to determine the absolute maximum strains. These were then multiplied by the appropriate moduli of elasticity to determine maximum live load stresses.

The bridge model was designed by the Bridge Department of the California Division of Highways using the "whole-width unit" concept described earlier. The allowable steel stress was 24.0 ksi to be produced by dead load, live load, and impact (22 percent for this bridge). For comparison, one can take 1.22 times the measured live load stresses given in Table 4 and add the nominal dead load stresses to see what total stresses are produced under two-lane AASHO truck loading, three-lane AASHO truck

Table 2. Theoretical and experimental reactions at east, center, and west supports.

Truck Position	No. of Lanes Loaded	No. of Spans Loaded	Theoretical Reaction (kip)			Experimental Reaction (kip)		
			East Support	Center Support	West Support	East Support	Center Support	West Support
3a + 4a	2	1	-1.4	12.3	7.1	-1.4	12.6	7.1
1a + 2a + 3a + 4a	2	2	5.7	24.6	5.7	5.4	24.3	5.7
4b + 5b + 6b	3	1	-2.1	18.4	10.7	-2.0	18.8	10.5
1b + 2b + 3b + 4b + 5b + 6b	3	2	8.6	36.8	8.6	8.2	36.8	8.6

Table 3. Maximum girder moments for vehicle loadings.

Section	Vehicle Positions	Maximum Girder Moments (ft-kip) M_{ext}	M_{int}	M_e/M_i
Two-Lane AASHO				
A	1a + 2a	16	21	0.76
B	1a + 2a + 3a + 4a	13	21	0.62
C	1a + 2a + 3a + 4a	13	20	0.65
D	3a + 4a	24	24	1.00
Three-Lane AASHO				
A	1b + 2b + 3b	21	30	0.70
B	1b + 2b + 3b + 4b + 5b + 6b	20	32	0.63
C	1b + 2b + 3b + 4b + 5b + 6b	20	29	0.69
D	4b + 5b + 6b	25	37	0.68
Construction Vehicle				
A	2c	36	54	0.67
B	1c + 3c	31	42	0.74
C	1c + 3c	21	49	0.65
D	4c	30	49	0.61

Figure 8. Experimental deflections at transverse midspan sections for various vehicle loadings.

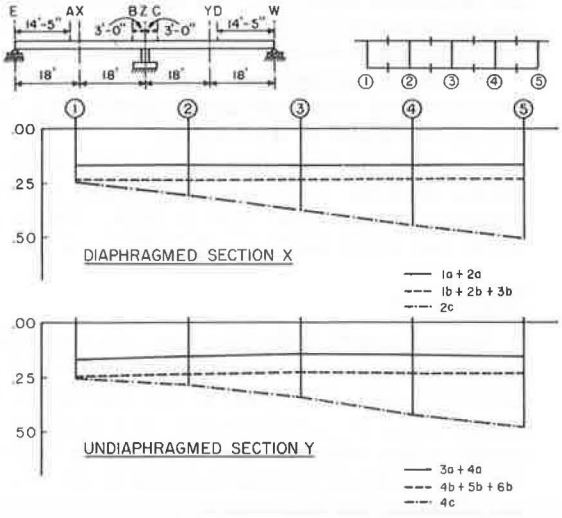

Table 4. Maximum live load experimental stresses for truck and construction vehicle loadings.

Material	Section	Two-Lane Truck Loading (psi)	Three-Lane Truck Loading (psi)	Construction Vehicle Loading (psi)
Concrete	A	207	276	516
	B	235	351	510
	C	241	346	514
	D	249	383	440
Steel	A	8,030	9,980	17,000
	B	3,710	5,850	10,200
	C	3,860	5,830	9,370
	D	6,640	10,700	13,000

loading, and one-lane overload construction vehicle loading. The nominal dead load stresses at positive moment sections A and D are 12.8 ksi and at negative moment sections B and C are 8.9 ksi. The resulting total stresses for the two-lane and three-lane AASHO truck loadings and the one-lane construction vehicle loading are 22.6, 25.9, and 33.5 ksi respectively at sections A and D and 13.6, 16.1, and 21.4 ksi at sections B and C, which are 3 ft from the centerline of the bent support. If the latter values are extrapolated to the centerline of the bent the total stresses are 21.3, 24.9, and 32.4 ksi.

The allowable concrete stress was 1.3 ksi. As can be seen from Table 4, the measured live load concrete stresses were quite low. The total concrete stresses at section A or D and B or C were below the allowable value; however, values extrapolated to the centerline of the bent were greater than the allowable value for the three-lane truck loading and the overload construction vehicle loading.

It is of interest to note from a design standpoint that, for both steel and concrete stresses, the dead load may contribute half or more to the total stress. Thus an error in the live load distribution factors of say 30 percent might give an error in the total stress of only 15 percent.

Finally, under all the vehicle loadings placed on the bridge, no visual signs of distress were observed. The crack patterns developed consisted of hairline cracks with widths of less than 0.01 in.

CONCLUSIONS

The most important conclusions from the study reported in this paper are as follows:

1. Both theoretical and experimental results show that for the bridge tested the AASHO empirical formula $N_{WL} = S/7$ overestimates the actual value of the girder moment slightly for a two-lane truck loading but underestimates it by as much as 23 percent for a three-lane truck loading on the bridge.
2. Concrete box girder bridges have excellent load-distributing properties because, under the most critical truck load positions, the transverse distribution of girder moments approaches that found for an optimum uniform stress distribution.
3. Steel and concrete stresses produced by dead load, live load, and impact are less than allowable values for two lanes of AASHO HS20-44 trucks but are greater for three lanes of AASHO HS20-44 trucks or for one lane of the class I proposed overload construction vehicle. However, none of these vehicle loadings produced any distress in the bridge.

ACKNOWLEDGMENT

This investigation was sponsored by the Division of Highways, State of California, and the Federal Highway Administration. The opinions, findings, and conclusions expressed are those of the writers and not necessarily those of the sponsors.

G. D. Mancarti and R. E. Davis of the Research and Development Section provided close liaison from the Bridge Department, Division of Highways, State of California.

REFERENCES

1. Bouwkamp, J. G., Scordelis, A. C., and Wasti, S. T. Structural Behavior of a Two Span Reinforced Concrete Box Girder Bridge Model, Volume 1. Univ. of California, Berkeley, Structural Eng. and Structural Mech. Rept. 71-5, April 1971.
2. Scordelis, A. C., Bouwkamp, J. G., and Wasti, S. T. Structural Behavior of a Two Span Reinforced Concrete Box Girder Bridge Model, Volume 2. Univ. of California, Berkeley, Structural Eng. and Structural Mech. Rept. 71-6, Oct. 1971.
3. Scordelis, A. C., Bouwkamp, J. G., and Wasti, S. T. Structural Behavior of a Two Span Reinforced Concrete Box Girder Bridge Model, Volume 3. Univ. of California, Berkeley, Structural Eng. and Structural Mech. Rept. 71-7, Oct. 1971.